Voltage-Dependent Photoluminescence and How It Correlates with the Fill Factor and Open-Circuit Voltage in Perovskite Solar Cells

Stolterfoht, Martin; Le Corre, Vincent M.; Feuerstein, Markus; Caprioglio, Pietro; Koster, L. Jan Anton; Neher, Dieter

Published in:
ACS Energy Letters

DOI:
10.1021/acsenergylett.9b02262

Publication date:
2019

ACS Energy LETTERS

Cite This: ACS Energy Lett. 2019, 4, 2887−2892

http://pubs.acs.org/journal/aelccp

LETTER

Voltage-Dependent Photoluminescence and How It Correlates with the Fill Factor and Open-Circuit Voltage in Perovskite Solar Cells

Martin Stolterfoht,*[,†] Vincent M. Le Corre,[‡] Markus Feuerstein,[†] Pietro Caprioglio,[†,§] L. Jan Anton Koster,[‡] and Dieter Neher*[,†]

[†]Institute of Physics and Astronomy, University of Potsdam, 14476 Potsdam, Germany

[‡]Zernike Institute for Advanced Materials, University of Groningen, Nijenborgh 4, 9747 AG Groningen, Netherlands

[§]Young Investigator Group Perovskite Tandem Solar Cells, Helmholtz-Zentrum Berlin für Materialien und Energie GmbH, Kekuléstraße 5, 12489 Berlin, Germany

Supporting Information

ABSTRACT: Optimizing the photoluminescence (PL) yield of a solar cell has long been recognized as a key principle to maximize the power conversion efficiency. While PL measurements are routinely applied to perovskite films and solar cells under open-circuit conditions (V_{OC}), it remains unclear how the emission depends on the applied voltage. Here, we performed PL(V) measurements on perovskite cells with different hole transport layer thicknesses and doping concentrations, resulting in remarkably different fill factors (FFs). The results reveal that PL(V) mirrors the current−voltage (JV) characteristics in the power-generating regime, which highlights an interesting correlation between radiative and nonradiative recombination losses. In particular, high FF devices show a rapid quenching of PL(V) from open-circuit to the maximum power point. We conclude that, while the PL has to be maximized at V_{OC}, at lower biases < V_{OC}, the PL must be rapidly quenched as charges need to be extracted prior to recombination.

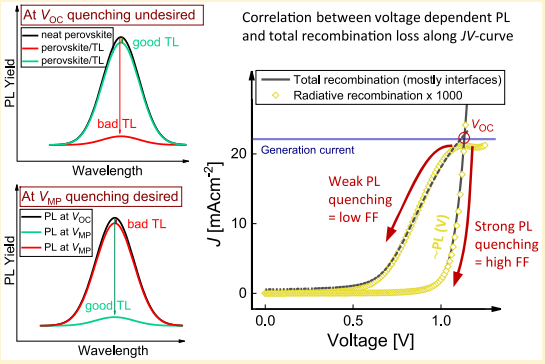

Within only 10 years of development, organic−inorganic perovskite solar cells caught up with their inorganic counterparts in terms of power conversion efficiency (PCE of 25.2%),[1] overpassing the best thin-film and multicrystalline silicon solar cells while getting close to the best monocrystalline silicon cells (26.7%).[2,3] However, this is not the end of the road as recent models predict a fundamental efficiency limit of above 30% even for single-junction perovskite cells.[4] Such efficiencies may be envisaged through further optimization of the charge transport layers (TLs) and reduction of nonradiative defect recombination at the interfaces and/or grain boundaries. Moreover, perovskites are highly relevant for a range of tandem applications, promising even higher performances, for example, all-perovskite tandem cells (reaching 24.8%),[5] four-terminal or monolithic tandem cells with silicon[6] (up to 28%)[1] or in combination with CIGS (23.3%).[7] Hence, understanding the mechanism and spatial location of the nonradiative losses remains an important task for the community.[8] In the ideal case, the internal quasi-Fermi level splitting (QFLS) in the perovskite absorber is equal to the external voltage and only limited by radiative recombination in the bulk. Measurement of the QFLS in the full device as a function of the external voltage will therefore provide information to which extent the situation differs from the ideal case. In this regard, photoluminescence (PL) measurements are becoming a popular tool in the community as they allow one to quantify the QFLS or the internal voltage in the neat perovskite, perovskite/TL stacks, or even complete solar cells.[9−12] This approach has been used to assess the quality of the neat material and recombination at interfaces and/or the metal contacts, while hyperspectral PL imaging is further beneficial when aiming to identify spatial inhomogeneities or device imperfections.[13,14] Moreover, intensity-dependent QFLS measurements have been recently performed to provide, for instance, access to the ideality factor of individual perovskite/TL junctions of the cell.[9,15] These studies have provided solid evidence regarding the limiting components of the cell as the emitted PL from an (unconnected) sample under open-circuit conditions (V_{OC}) is only reduced by nonradiative recombination processes that

Received: October 16, 2019
Accepted: October 28, 2019
Published: October 28, 2019

DOI: 10.1021/acsenergylett.9b02262
ACS Energy Lett. 2019, 4, 2887−2892

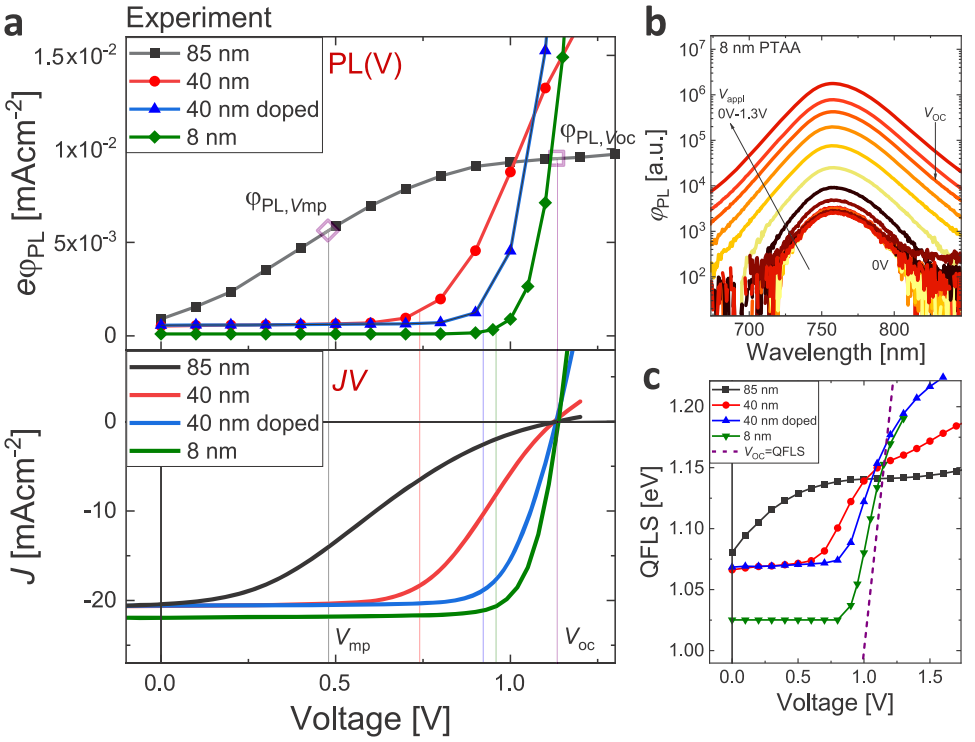

Figure 1. (a) Voltage-dependent PL yield ($\phi_{PL}(V)$) and *JV* curves measured on p−i−n type cells with a PTAA bottom TL with variable thickness. While the PL should be maximized at V_{OC}, in forward bias, charges must be swiftly extracted from the device and the PL be rapidly quenched. The graph highlights the correlation between the *JV* curve, which is shaped through nonradiative losses, and the radiative recombination loss ($J_{rad}(V) = e\phi_{PL}(V)$). (b) Voltage-dependent PL spectra of the cell with 8 nm PTAA. (c) QFLS as a function of external applied voltage in the devices with different PTAA layer thicknesses highlighting a significant internal voltage in the perovskite layer at low applied voltages potentially causing voltage-independent short-circuit current losses.

lower the QFLS throughout the stack. In fact, the absolute intensity of the emitted PL yield (ϕ_{PL}), or equivalently the radiative recombination current density ($J_{rad} = \phi_{PL}/e$), depends logarithmically on the QFLS (μ) in the junction.[9−12]

$$e\phi_{PL} = J_{rad} = J_{0,rad} \exp(\mu/k_B T) \quad (1)$$

where $J_{0,rad}$ is the radiative thermal recombination current density in the dark (see Supplementary Note 1 for further details and assumptions). Equation 1 shows that a low PL yield always corresponds to a low internal voltage or QFLS. We note that in the perovskite literature it is common to find that under V_{OC} conditions PL quenching is a desirable property of a TL as it would imply efficient charge transfer and extraction from the perovskite to the TLs.[16,17] This misconception probably has its origin from organic solar cell research where the quenching of the PL in bulk-heterojunction blends meant efficient exciton dissociation.[18] However, in perovskites, where excitons usually dissociate immediately after photogeneration at room temperature,[19,20] this is irrelevant, and the subsequent quenching of radiative recombination always corresponds to a lower QFLS. Here, it is interesting to note that, even at V_{OC}, the cell might not be in a generation−recombination equilibrium at every point in the device. For example, nonradiative recombination at the interface between the perovskite and the TL will cause a flow of electrons and holes in the active layer toward this interface, but these currents will cancel each other out, resulting in an external current of 0 at V_{OC}. Therefore, when considering two perovskite/TL films where the TLs exhibit identical recombination but different extraction properties, it may still be that the superior extraction capability of one TL leads to a stronger PL quenching. However, this only means that the faster extraction enhances the nonradiative recombination loss in a particular region of the sample, which is detrimental for the V_{OC}. Notwithstanding these points, it is important to emphasize that the above considerations are valid only under open-circuit conditions. In the power-generating regime below the V_{OC}, the situation is expected to be markedly different as ideally, photogenerated charges are extracted out of the perovskite layer prior to recombination. Consequently, in this regime, the PL should be rapidly quenched as the free charge carrier population (which leads to the PL emission) should be as low as possible to avoid any type of recombination. However, until today, PL measurements were usually limited to the study of cells and/or films under open-circuit conditions.

In this work, we extended the framework of the PL-QFLS methodology by studying the bias dependence of the PL on triple-cation-based perovskite solar cells with varying hole transport layer (HTL) thicknesses and amount of F4TCNQ doping, while the results are also generalized to n−i−p cells with C_{60} and P3HT as electron and hole transport layers (ETL/HTL), respectively. We demonstrate that the voltage dependence of the PL mirrors the shape of current density vs voltage (*JV*) characteristics, highlighting the correlation between radiative and nonradiative recombination losses. A figure of merit is proposed that is based on the quenching factor of the ϕ_{PL} from open-circuit to the maximum power point (V_{mp} or MPP) as a sensitive measure for the extraction capability and the fill factor (FF) of the cell.

DOI: 10.1021/acsenergylett.9b02262
ACS Energy Lett. 2019, 4, 2887−2892

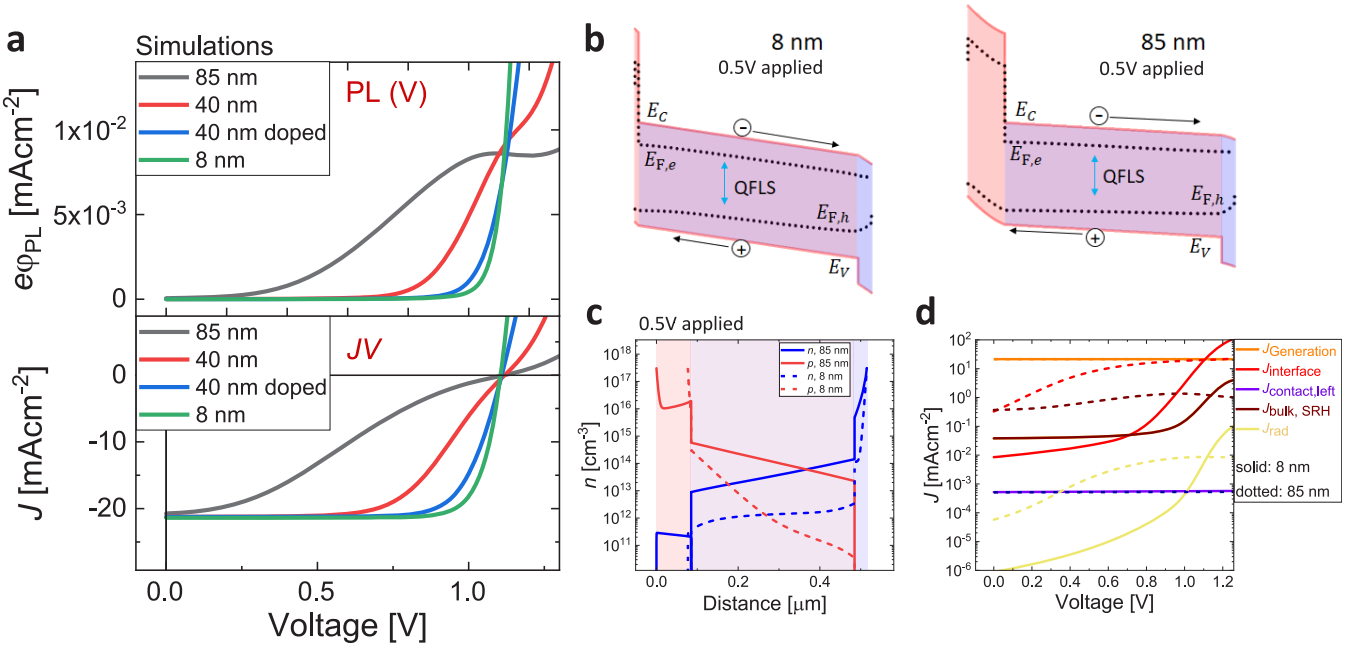

Figure 2. (a) Numerically simulated radiative recombination current ($e\phi_{PL}(V)$) and corresponding *JV* curves in analogy to the experimental results in Figure 1a. (b) Exemplified band diagrams of a device with a thin (8 nm) and a thick (85 nm) TL at an applied voltage of 0.5 V. The considerable built-in voltage drop over the thick, resistive PTAA layer (85 nm) leads to flat energy bands in the perovskite layer at quite low applied voltages. As shown in panel (c), this causes more charge accumulation in the active layer (hence more PL) but also leads to a higher concentration of minority carriers at the interfaces (i.e., holes as the perovskite/ETL interface). (d) Resulting voltage-dependent recombination currents in p−i−n type perovskite solar cells with a thick (85 nm) and a thin (8 nm) PTAA layer. The reason for the reduced FF in the cell with the thick PTAA layer is the increased interfacial recombination current at the perovskite/ETL interface (red lines), which happens at lower applied voltages due to the resistive TL and the reduced potential drop across the perovskite. For example, at an applied voltage of 0.5 V, the interfacial recombination current is ∼350 times larger in the cell with the thick PTAA layer than that in the cell with the thin layer.

The cells studied in this work are characterized by a remarkably different FF, as highlighted in a previous study, due to the charge transport limitation imposed by the low-mobility PTAA layer.[21,22] The voltage-dependent PL yield of the devices and the corresponding *JV*-curves are shown in Figure 1a, while Figure 1b exemplifies the original PL spectra from 0 to 1.4 V applied for the cell with the thinnest PTAA layer (8 nm). We note that all measured devices exhibit a similar V_{OC} irrespective of the HTL thickness/doping and show a similar PL intensity under V_{OC} conditions, as expected from eq 1. Importantly, the PL emission correlates well with the FF of the devices, that is, the lower the emission in the power-generating regime, the higher the FF. As such, the device with the 85 nm thick PTAA layer has already a considerable emission at low biases due to significant bimolecular recombination of accumulated charges within the active layer.[21,22] For this device, charge extraction is so inefficient that the charge carrier density in the active layer remains essentially close to the situation at open-circuit conditions even at comparatively low applied biases. The behavior of the cell with the thick PTAA layer is in sharp contrast to the device with the thin or doped PTAA TL where the PL emission is comparatively low at the MPP. This effect can be partially understood considering the Shockley equation with an effective transport resistance (R_{tr}), $J_L = -J_G + J_0\,[\exp(q(V_{appl} - J_L R_{tr})/k_B T) - 1]$, where J_L, J_G, and J_0 are the light, generation, and dark saturation currents, respectively. The resistance of the TL, R_{tr}, leads to a higher internal voltage across the active layer than externally applied (V_{appl}) and consequently to more recombination losses.[23,24] This is further shown in Figure 1c, where we quantified the QFLS or the internal voltage in the perovskite as a function of bias voltage using the voltage-dependent PL. This demonstrates that it is only the device with the very thin PTAA layer that obeys the Shockley−Queisser condition QFLS = qV_{OC} at a bias close to V_{OC}. It is also clear that all cells exhibit a large internal voltage that saturates above 1 V when decreasing the applied voltage to 0 V. We note that this may indicate the presence of small, unconnected regions in the volume of the active pixel, which could potentially dominate the emission at low biases. Notably, this may also explain the small voltage-independent short-circuit current losses in our devices and more generally charge collection losses at 0 V that are quite often observed in perovskite solar cells.[25] While this observation will require more high-resolution PL measurements and analysis in the future, in this work, we aim at studying the emission at applied voltages above the QFLS saturation.

To describe the experiments more quantitatively, we performed drift-diffusion simulations using the open-source software SCPAS.[26] The simulations include several important previously measured material and device parameters, such as the carrier mobilities in the layers,[22,27] interfacial and bulk lifetimes,[12] energy levels,[8] as well as the recombination rate constants in the perovskite and density of states in the perovskite.[28] The simulation parameters are shown in Table S1. For example, using the experimentally obtained values for the interface recombination velocity (S = 200 cm/s at the HTL/perovskite interface and S = 2000 cm/s at the perovskite/ETL interface) and the bulk lifetime (∼500 ns),[12] we can well reproduce the ideality factor of the optimized cells

DOI: 10.1021/acsenergylett.9b02262
ACS Energy Lett. 2019, 4, 2887−2892

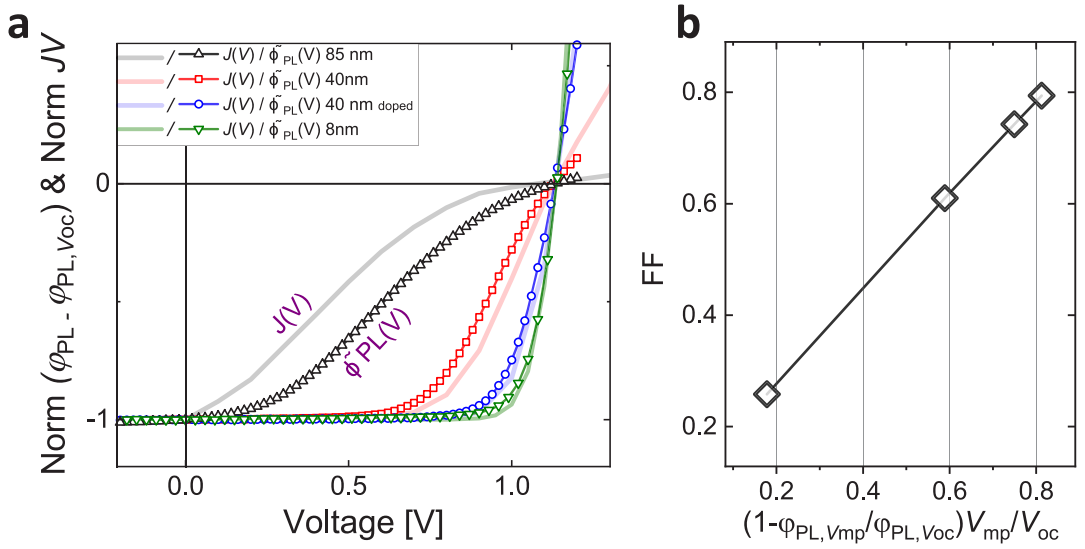

Figure 3. (a) Normalized *JV* and pseudo-*JV* curves ($\tilde{\phi}_{PL}(V)$) of the PTAA-based p−i−n type cells shown in Figure 1a. The pseudo-*JV* curves were obtained by subtracting the PL yield at open-circuit conditions ($\phi_{PL,V_{OC}}$) from the bias-dependent photoluminescence PL(V). The curves represent hypothetical *JV* curves that are impacted by only radiative recombination but with the same V_{OC} as the actual *JV* curves, i.e., $J_L = -J_{rad,V_{OC}} + J_{rad}(V)$. (b) Device FF vs the proposed FOM from the voltage-dependent PL (1 minus the PL quenching ratio from V_{OC} to V_{mp} times V_{mp}/V_{OC}). The PL at V_{mp} and V_{OC} was taken as indicated by the lines in Figure 1a. The graph underlines the correlation between radiative and nonradiative recombination losses in the power-generating *JV* regime.

with the 8 nm thick PTAA layer as well as the experimentally measured recombination currents in the neat perovskite and the interfaces under open-circuit conditions (Figure S1). We note that the recombination currents were obtained using steady-state PL/QFLS measurements.[8] Figure 2a shows the results of the drift diffusion simulations, which can well reproduce the observed experimental dependence of J_{rad} and J_L on the applied voltage in a linear representation. Figure 2b exemplifies the band diagrams of a cell with a thick (85 nm) and thin (8 nm) TL at V_{appl} = 0.5 V, which shows that a large fraction of the remaining built-in voltage drops across the thick PTAA layer, reducing the internal field across the perovskite layer. Figure 2c shows that this leads to a higher charge carrier density in the active layer but also a higher minority carrier density at the interfaces. This, in turn, accelerates the nonradiative interfacial recombination losses, as shown in Figure 2d, and explains the observed correlation between the radiative and nonradiative losses in the power-generating *JV* regime.

Considering again the similarity of the voltage-dependent PL in Figure 1a and the corresponding *JV* curves, which are shaped by the total recombination current ($J_L = -J_G + J_{R,tot}$), suggests that J_{rad} and $J_{R,tot}$ are related. In order to directly compare $J_{rad}(V)$ and $J_{R,tot}(V)$, we shift the voltage-dependent PL data shown in Figure 1a into the fourth quadrant by simply subtracting the radiative recombination current at V_{OC} from $\phi_{PL}(V)$, i.e., $e\tilde{\phi}_{PL}(V) = e\phi_{PL}(V) - e\phi_{PL,V_{OC}}$. This effectively creates a pseudo-*JV* curve, $\tilde{\phi}_{PL}(V)$, that is limited only by radiative recombination but exhibits the same V_{OC} as that in the actual *JV* measurement. The pseudo- and the actual *JV* curves normalized to the current at 0 V are shown in Figure 3a. In order to quantitatively correlate $\tilde{\phi}_{PL}(V)$ and the *JV* curve, we express the FF of the pseudo-*JV* curve ($\widetilde{FF}_{PL}$) in analogy with the common expression of the FF [$FF = (J_{mp}/J_{SC})\cdot(V_{mp}/V_{OC})$]

$$\widetilde{FF}_{PL} = (\tilde{J}_{mp}/e\phi_{PL,V_{OC}})\cdot(V_{mp}/V_{OC}) = (1 - e\phi_{PL,V_{mp}}/e\phi_{PL,V_{OC}})(V_{mp}/V_{OC}) \quad (2)$$

Note that the terms in brackets represent the normalized current of photogenerated charges surviving radiative recombination at V_{mp} (analogous to J_{mp}/J_{SC} in a normal *JV* curve). In Figure 3b, we then plot the actual FF versus $\widetilde{FF}_{PL}$, which highlights the correlation between the radiative and nonradiative losses in the power generating *JV* regime. Moreover, this shows that $\widetilde{FF}_{PL} = (1 - e\phi_{PL,V_{mp}}/e\phi_{PL,V_{OC}})(V_{mp}/V_{OC})$ may also be used as a figure of merit (FOM) to predict the FF of a perovskite solar cell from the quenching ratio of the PL from V_{OC} to MPP conditions (this is exemplified in Figure 1a for the cell with the thick PTAA layer). We further note that a corresponding analysis and plot for the P3HT-based n−i−p type cells is shown in the Figure S2. Overall, this analysis demonstrates that high FFs can only be achieved if the PL emission from the active layer is rapidly reduced when decreasing the external voltage below V_{OC}. We also note that the voltage-dependent PL data was taken at a scan rate of 5−10 mV/s (Supplementary Methods) under which the cells studied herein exhibit no relevant hysteresis in the power-generating *JV* regime (Figure S3). Therefore, the correlation between the PL(V) and the *JV* curve is not influenced by the motion of ions in our cells. However, we note that any hysteresis in the *JV* scan is expected to produce a similar hysteresis in J_{rad}. Finally, as an outlook, we anticipate that in the near future, precise measurements and modeling of bias-dependent PL and QFLS will provide important insights into the carrier density in the active layer and, for example, the built-in voltage drop across the perovskite layer under short-circuit conditions.

In summary, in this Letter, we have discussed why the PL emission from a perovskite cell or a perovskite/TL junction

DOI: 10.1021/acsenergylett.9b02262
ACS Energy Lett. 2019, 4, 2887−2892

should be maximized by all means under open-circuit conditions yet minimized in the power-generating *JV* regime as the charge carrier density in the active layer should be as low as possible to guarantee a low recombination rate. As such, we demonstrated that devices with high FFs stand out by a rapid quenching of the PL when moving from the V_{OC} to the MPP. Following this line of argument, we proposed a FOM for the FF that is based on quenching of the PL under MPP conditions with respect to the PL under open-circuit. The conclusions were validated for two types of perovskite solar cells with PCEs of up to 20%. Moreover, we found that most devices exhibited a saturated high internal QFLS (1 eV) at low applied voltages (Figure 1c), which could be one reason for the J_{SC} being sometimes lower than expected for a given band gap considering realistic reflection/parasitic absorption losses. We anticipate that high-precision voltage-dependent PL measurements will provide further insights into the electrostatic potential and charge carrier distribution in perovskite solar cells in the near future.

■ ASSOCIATED CONTENT

Supporting Information

The Supporting Information is available free of charge on the ACS Publications website at DOI: 10.1021/acsenergylett.9b02262.

Methods section, a table with simulation parameters, a fit of simulations to several experimental data (intensity-dependent V_{OC} and nonradiative recombination currents), PL(V)/JV analysis of n−i−p type cells with C_{60} and P3HT as charge transport layers, and hysteresis scans of the cells shown in the main text (PDF)

■ AUTHOR INFORMATION

Corresponding Authors

*E-mail: stolterf@uni-potsdam.de.
*E-mail: neher@uni-potsdam.de.

ORCID

Martin Stolterfoht: 0000-0002-4023-2178
Vincent M. Le Corre: 0000-0001-6365-179X
L. Jan Anton Koster: 0000-0002-6558-5295
Dieter Neher: 0000-0001-6618-8403

Notes

The authors declare no competing financial interest.
The data that support the plots within this paper and other findings of this study are available from the corresponding authors upon reasonable request.

■ ACKNOWLEDGMENTS

This work was in part funded by HyPerCells (a joint graduate school of the Potsdam University and the HZB) and by the Deutsche Forschungsgemeinschaft (DFG, German Research Foundation) - project number 423749265. The work by V.M.L.C. was supported by a grant from STW/NWO (VIDI 13476).

■ REFERENCES

(1) NREL. Best Research-Cell Efficiencies. https://www.nrel.gov/pv/cell-efficiency.html (accessed Sept 2, 2019).
(2) Yamamoto, K.; Yoshikawa, K.; Uzu, H.; Adachi, D. High-Efficiency Heterojunction Crystalline Si Solar Cells. *Jpn. J. Appl. Phys.* **2018**, *57* (8S3), 08RB20.
(3) Yoshikawa, K.; Kawasaki, H.; Yoshida, W.; Irie, T.; Konishi, K.; Nakano, K.; Uto, T.; Adachi, D.; Kanematsu, M.; Uzu, H.; et al. Silicon Heterojunction Solar Cell with Interdigitated Back Contacts for a Photoconversion Efficiency over 26%. *Nat. Energy* **2017**, *2* (5), 17032.
(4) Pazos-Outón, L. M.; Xiao, T. P.; Yablonovitch, E. Fundamental Efficiency Limit of Lead Iodide Perovskite Solar Cells. *J. Phys. Chem. Lett.* **2018**, *9* (7), 1703−1711.
(5) Lin, R.; Xiao, K.; Qin, Z.; Han, Q.; Zhang, C.; Wei, M.; Saidaminov, M. I.; Gao, Y.; Xu, J.; Xiao, M.; et al. Monolithic All-Perovskite Tandem Solar Cells with 24.8% Efficiency Exploiting Comproportionation to Suppress Sn(Ii) Oxidation in Precursor Ink. *Nat. Energy* **2019**, *4* (10), 864−873.
(6) Sahli, F.; Werner, J.; Kamino, B. A.; Bräuninger, M.; Monnard, R.; Paviet-Salomon, B.; Barraud, L.; Ding, L.; Diaz Leon, J. J.; Sacchetto, D.; et al. Fully Textured Monolithic Perovskite/Silicon Tandem Solar Cells with 25.2% Power Conversion Efficiency. *Nat. Mater.* **2018**, *17* (9), 820−826.
(7) Al-Ashouri, A.; Magomedov, A.; Roß, M.; Jošt, M.; Talaikis, M.; Chistiakova, G.; Bertram, T.; Márquez, J. A.; Köhnen, E.; Kasparavičius, E.; et al. Conformal Monolayer Contacts with Lossless Interfaces for Perovskite Single Junction and Monolithic Tandem Solar Cells. *Energy Environ. Sci.* **2019**, DOI: 10.1039/C9EE02268F.
(8) Stolterfoht, M.; Caprioglio, P.; Wolff, C. M.; Márquez, J. A.; Nordmann, J.; Zhang, S.; Rothhardt, D.; Hörmann, U.; Amir, Y.; Redinger, A.; et al. The Impact of Energy Alignment and Interfacial Recombination on the Internal and External Open-Circuit Voltage of Perovskite Solar Cells. *Energy Environ. Sci.* **2019**, *12* (9), 2778−2788.
(9) Sarritzu, V.; Sestu, N.; Marongiu, D.; Chang, X.; Masi, S.; Rizzo, A.; Colella, S.; Quochi, F.; Saba, M.; Mura, A.; et al. Optical Determination of Shockley-Read-Hall and Interface Recombination Currents in Hybrid Perovskites. *Sci. Rep.* **2017**, *7* (1), 44629.
(10) El-Hajje, G.; Momblona, C.; Gil-Escrig, L.; Avila, J.; Guillemot, T.; Guillemoles, J.-F.; Sessolo, M.; Bolink, H. J.; Lombez, L. Quantification of Spatial Inhomogeneity in Perovskite Solar Cells by Hyperspectral Luminescence Imaging. *Energy Environ. Sci.* **2016**, *9* (7), 2286−2294.
(11) Wu, N.; Wu, Y.; Walter, D.; Shen, H.; Duong, T.; Grant, D.; Barugkin, C.; Fu, X.; Peng, J.; White, T.; et al. Identifying the Cause of Voltage and Fill Factor Losses in Perovskite Solar Cells by Using Luminescence Measurements. *Energy Technol.* **2017**, *5* (10), 1827−1835.
(12) Stolterfoht, M.; Wolff, C. M.; Márquez, J. A.; Zhang, S.; Hages, C. J.; Rothhardt, D.; Albrecht, S.; Burn, P. L.; Meredith, P.; Unold, T.; et al. Visualization and Suppression of Interfacial Recombination for High-Efficiency Large-Area Pin Perovskite Solar Cells. *Nat. Energy* **2018**, *3* (10), 847−854.
(13) Braly, I. L.; Hillhouse, H. W. Optoelectronic Quality and Stability of Hybrid Perovskites from MAPbI3 to MAPbI2Br Using Composition Spread Libraries. *J. Phys. Chem. C* **2016**, *120* (2), 893−902.
(14) El-Hajje, G.; Momblona, C.; Gil-Escrig, L.; Ávila, J.; Guillemot, T.; Guillemoles, J.-F.; Sessolo, M.; Bolink, H. J.; Lombez, L. Quantification of Spatial Inhomogeneity in Perovskite Solar Cells by Hyperspectral Luminescence Imaging. *Energy Environ. Sci.* **2016**, *9*, 2286−2294.
(15) Caprioglio, P.; Stolterfoht, M.; Wolff, C. M.; Unold, T.; Rech, B.; Albrecht, S.; Neher, D. On the Relation between the Open-Circuit Voltage and Quasi-Fermi Level Splitting in Efficient Perovskite Solar Cells. *Adv. Energy Mater.* **2019**, *9* (33), 1901631.
(16) Cao, J.; Mo, S.; Jing, X.; Yin, J.; Li, J.; Zheng, N. Trace Surface-Clean Palladium Nanosheets as a Conductivity Enhancer in Hole-Transporting Layers to Improve the Overall Performances of Perovskite Solar Cells. *Nanoscale* **2016**, *8* (6), 3274−3277.
(17) Salado, M.; Idigoras, J.; Calio, L.; Kazim, S.; Nazeeruddin, M. K.; Anta, J. A.; Ahmad, S. Interface Play between Perovskite and Hole Selective Layer on the Performance and Stability of Perovskite Solar Cells. *ACS Appl. Mater. Interfaces* **2016**, *8*, 34414.

DOI: 10.1021/acsenergylett.9b02262
ACS Energy Lett. 2019, 4, 2887−2892

(18) Baran, D.; Li, N.; Breton, A.-C.; Osvet, A.; Ameri, T.; Leclerc, M.; Brabec, C. J. Qualitative Analysis of Bulk-Heterojunction Solar Cells without Device Fabrication: An Elegant and Contactless Method. *J. Am. Chem. Soc.* **2014**, *136* (31), 10949−10955.
(19) Lin, Q.; Armin, A.; Nagiri, R. C. R.; Burn, P. L.; Meredith, P. Electro-Optics of Perovskite Solar Cells. *Nat. Photonics* **2015**, *9* (2), 106−112.
(20) Miyata, A.; Mitioglu, A.; Plochocka, P.; Portugall, O.; Wang, J. T.; Stranks, S. D.; Snaith, H. J.; Nicholas, R. J. Direct Measurement of the Exciton Binding Energy and Effective Masses for Charge Carriers in Organic-Inorganic Tri-Halide Perovskites. *Nat. Phys.* **2015**, *11* (7), 582−587.
(21) Le Corre, V. M.; Stolterfoht, M.; Perdigón Toro, L.; Feuerstein, M.; Wolff, C.; Gil-Escrig, L.; Bolink, H. J.; Neher, D.; Koster, L. J. A. Charge Transport Layers Limiting the Efficiency of Perovskite Solar Cells: How To Optimize Conductivity, Doping, and Thickness. *ACS Appl. Energy Mater.* **2019**, *2* (9), 6280−6287.
(22) Stolterfoht, M.; Wolff, C. M.; Amir, Y.; Paulke, A.; Perdigón-Toro, L.; Caprioglio, P.; Neher, D. Approaching the Fill Factor Shockley−Queisser Limit in Stable, Dopant-Free Triple Cation Perovskite Solar Cells. *Energy Environ. Sci.* **2017**, *10* (6), 1530−1539.
(23) Würfel, U.; Neher, D.; Spies, A.; Albrecht, S. Impact of Charge Transport on Current-Voltage Characteristics and Power-Conversion Efficiency of Organic Solar Cells. *Nat. Commun.* **2015**, DOI: 10.1038/ncomms7951.
(24) Neher, D.; Kniepert, J.; Elimelech, A.; Koster, L. J. A. A New Figure of Merit for Organic Solar Cells with Transport-Limited Photocurrents. *Sci. Rep.* **2016**, *6*, 24861.
(25) Liu, Z.; Krückemeier, L.; Krogmeier, B.; Klingebiel, B.; Márquez, J. A.; Levcenko, S.; Öz, S.; Mathur, S.; Rau, U.; Unold, T.; et al. Open-Circuit Voltages Exceeding 1.26 V in Planar Methylammonium Lead Iodide Perovskite Solar Cells. *ACS Energy Lett.* **2019**, *4* (1), 110−117.
(26) Burgelman, M.; Nollet, P.; Degrave, S. Modelling Polycrystalline Semiconductor Solar Cells. *Thin Solid Films* **2000**, *362*, 527−532.
(27) Herz, L. M. Charge-Carrier Mobilities in Metal Halide Perovskites: Fundamental Mechanisms and Limits. *ACS Energy Lett.* **2017**, *2* (7), 1539−1548.
(28) Staub, F.; Hempel, H.; Hebig, J. C.; Mock, J.; Paetzold, U. W.; Rau, U.; Unold, T.; Kirchartz, T. Beyond Bulk Lifetimes: Insights into Lead Halide Perovskite Films from Time-Resolved Photoluminescence. *Phys. Rev. Appl.* **2016**, *6* (4), 1−13.

DOI: 10.1021/acsenergylett.9b02262
ACS Energy Lett. 2019, 4, 2887−2892